Rayleigh scattering in X-ray polarimetry

Andrey Bondarev

Saint-Petersburg State University, b.ndarev@gmail.com

In this report we present experimental investigations of Rayleigh scattering for high energy X-rays and its relevance for X-ray polarimetry. Using radiation from the European Synchrotron Radiation Facility in Grenoble and a two-dimensial position sensitive microstrip Ge(i) X-ray detector, we were able to identify and study the Rayleigh scattering process together with Compton scattering.

1 Introduction

The measurement of linear polarization for hard X-rays by means of Compton scattering and segmented detectors is a well-established technique [1]. However, at photon energies lower than ≈ 100 keV the high photoelectric absorption cross-sections and small electron recoils reduce the efficiency of active scattering targets. Here one can possibly use Rayleigh scattering to analyze photon linear polarization. In the following we will present experimental study of Rayleigh scattering in a 2D microstrip germanium detector.

Fig. 1: *Cross-section for the main interaction processes of hard X-rays with germanium atoms.*

2 Rayleigh scattering

Photons scattering off bound electrons deposit little energy to the recoiling atom. Energy and momentum conservation yield the following kinematical relation between the scattered photon energy $\hbar\omega'$ and the scattering angle θ:

$$\hbar\omega' = \hbar\omega \frac{1}{1 + \frac{\hbar\omega}{Mc^2}(1 - \cos\theta)}, \quad (1)$$

where $\hbar\omega$ is the initial energy of photon and M is the mass of the atom. In most of the cases, the photon energy is much smaller than the rest energy of an atom, thus $\hbar\omega' \approx \hbar\omega$. Therefore, Rayleigh-based polarimetry might serve as a unique polarimetry method with a spectroscopic resolution limited only by the energy resolution of the applied detectors. Fig. 1 shows the cross-sections for various photon interaction processes in germanium. Here one can see that at energies below 70 keV Rayleigh scattering dominates over Compton scattering.
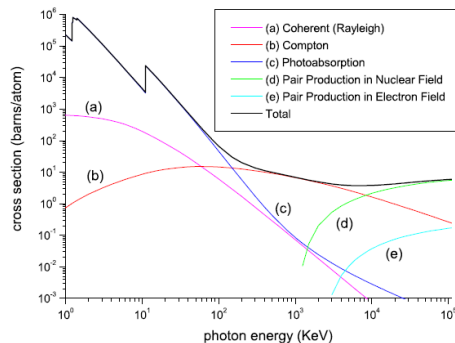
A linear polarization of the incoming photons results in an intensity modulation of the radiation scattered at an azimuthal angle φ with respect to the polarization vector [2] (see Fig. 2):

$$I(\varphi) \sim M \cdot P \cdot \sin^2\varphi + (1/2)(1 - M \cdot P), \quad (2)$$

where P is the degree of linear polarization and M is a modulation function. Therefore, one can obtain the degree of linear polarization via measurements of angular distribution around the scattering center.

For 100% polarized light

$$M = \frac{I(90) - I(0)}{I(90) + I(0)}. \quad (3)$$

It depends on the scattering angle θ and reaches its maximum at $\theta = 90°$. In any form-factor approximation theory, the modulation is independent of the target atom and photon energy and

is given by [3]

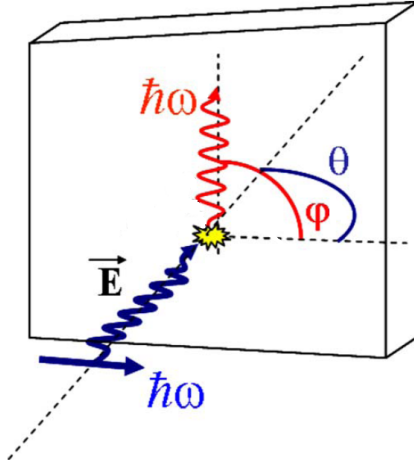$$M = \frac{1 - \cos^2\theta}{1 + \cos^2\theta}.\qquad(4)$$

Fig. 2: *Rayleigh scattering. A photon of energy $\hbar\omega$ is scattered on an atom under an angle of θ with respect to its original direction. The azimuthal angle φ gives the direction of the scattered photon with respect to the polarization vector $\vec{E}$.*

3 Detector

As a detector, a single crystal of high purity *n*-type germanium with a total area of 41×70 mm^2 and a thickness of 11 mm has been used (see Fig. 3) [4]. The front side consists of a boron implanted p^+ contact. It is divided by plasma etching into 128 strips of length 56 mm and pitch 250 μm. The strips are separated by 28 μm wide, and 15 μm deep, grooves. The back side is an amorphous Ge contact, which has beed segmented by plasma etching into 48 strips. These strips have a length of 32 mm with a pitch of 1167 μm and are oriented perpendicular to the strips on the front side. The active area of 32×56 mm^2 is surrounded by a guard ring of approximately 8 mm width to isolate and drain leakage currents.

Taking the front side and the back side strips together, the detector can thus be divided into 128×48 pixels (see Fig. 4). This provides a 2D-position sensitivity. We note that these pixels, obtained by combination of the front side and back side strips are not square. The reason for the unequal sizes of the front and back strips is that the detector was mainly designed to be
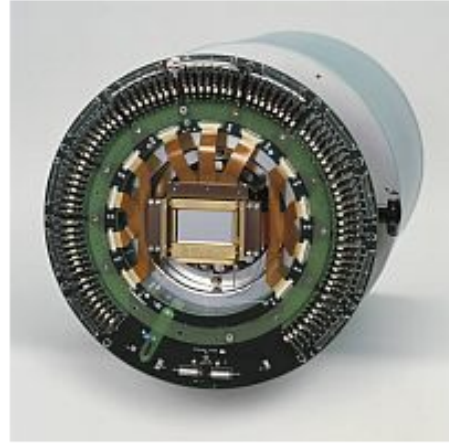

Fig. 3: *The germanium detector used in this study.*

used together with the crystal spectrometer [5]. This requires a very good position resolution in the direction of the dispersion given by the 250 μm wide strips, whereas the position resolution in the orthogonal direction is not as significant. Each strip is read out separately with a charge sensitive preamplifier. On the front side, the positive charge carriers and on the back side, the negative charge carriers, are collected. The energy information is thus obtained for each strip in the front and back sides. In the measurements reported here, all 48 back side strips and 64 of the 128 front side strips have been separately connected to the readout electronics, enabling the coincident readout of the connected strips. The remaining 64 frontside strips were not read out.
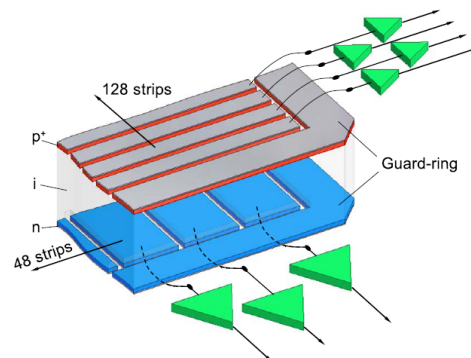

Fig. 4: *Schematic drawing of a small section of the Ge(i) crystal with etched orthogonal strips on front (p) and back (n) sides surrounded by a guard ring. Each strip is furnished with a separate readout.*

4   Results

For our study we used a Ge-microstrip detector and a well focused (∼50 μm in diameter) X-ray beam at the European Synchrotron Radiation Facility (ESRF)[1]. Since our detector has reasonable energy and time resolutions together with position sensitivity, it can be used to identify Compton and Rayleigh scattering processes. In these measurements, the beam was focused on a single pixel. The spectrum of incident radiation on this pixel (see Fig. 5) has three lines. The first is low-energy noise and the second and the third are at 70 keV and 210 keV, respectively. In other pixels, scattered photons were registered. Before analyzing the obtained data,
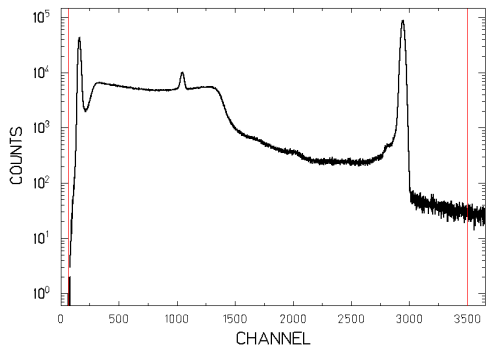

Fig. 5: *Uncalibrated energy spectrum of synchrotron radiation received by the 2D detector.*

one has to do an energy calibration of the detector. This means that we need to determine correspondence between energy and channel for each strip. Thus, after measurements with synchrotron radiation, the whole detector was irradiated by a $^{133}_{56}$Ba source with very well known X-ray lines. Then, for every strip, we plot a linear dependence of energy against channel. It is a linear dependence so we need at least three lines. Unfortunately, in our energy range, there are only three strong barium lines which we can use for calibration: at 30 keV, 35 keV and 80 keV. So calibration at large energies (we are also interested in the peak at 210 keV) is not so good because all the barium calibration lines we used are at much lower energy and therefore, uncertainty in the calibration at 210 keV is quite large. Obtained data was analyzed by means of a special package, SATAN[2] (System for the analysis of tremendous amounts of nuclear data). It

requires a program code in PL/I[3]. In order to detect Rayleigh scattered photons, we require only one event in the whole detector with the energy laying close to the peak's energy. In addition, the pixel where the event was registered should not be the pixel that the primary photon beam was focused on. We have considered scattered photons with energies close to 70 keV and close to 210 keV. On Fig. 6, we show a spectrum of Rayleigh scattered photons with initial energy close to 70 keV (events whose multiplicity equals unity, which were registered not in the pixel where the primary photon beam was focused and with energies close to 70 keV). The peak corresponds to Rayleigh scattering of 70 keV photons in our detector.
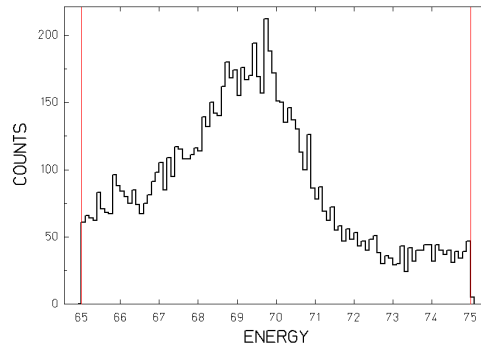

Fig. 6: *Spectrum of Rayleigh scattered photons with inicial energy close to 70 keV .*

Next, the obtained 2D distribution (see Fig. 7) was projected on the φ-axis (see Fig. 2) and was fitted to the function

$$I(\varphi) = A \cdot (M \cdot \sin^2 \varphi + (1/2)(1 - M)) \quad (5)$$

having the modulation function M (compare with Eqn. 2: $P \approx 1$, as we used almost 100% polarized synchrotron radiation) and the amplitude A as free parameters (see Fig. 8). The fit-
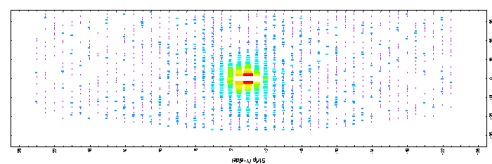

Fig. 7: *Position distribution of Rayleigh scattered photons for energy range 70 keV ± 5 keV.*

ting of the intensity modulation curves yielded $M = 0.45 \pm 0.06$ and $M = 0.39 \pm 0.08$ for the

[1] www.esrf.eu

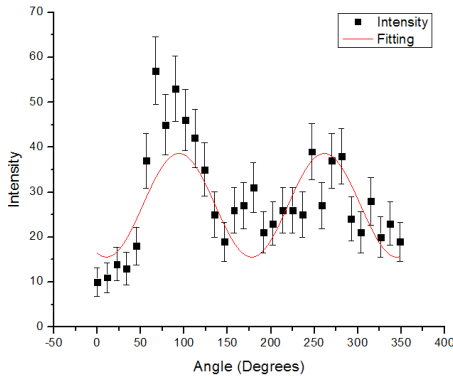[2] www-wnt.gsi.de/CHARMS/SATAN/graf.htm

[3] www-01.ibm.com/.../pli/

Fig. 8: *Projection of the position distribution on the φ-axis together with the least square fit of Eqn. 5.*

energies of 70 keV and 210 keV respectively. The asymmetry between scattering at 90° and 270° is most probably due to the fact that the incoming beam is not well centered on the central pixel. Here, we like to note that these results for the modulation factor can not be directly compared with a theory (see Eqn. 4), because in our setup the scattering angle θ can not be fixed. This is due to the relatively large thickness of the detector. Note that in the case of Compton scattering, θ can be fixed by applying energy conditions according to Compton kinematics. As a comparison, on Fig. 9, we present the angular modulation of the intensity corresponding to Compton scattering of 210 keV photons at the angle $\theta = 90° \pm 15°$.
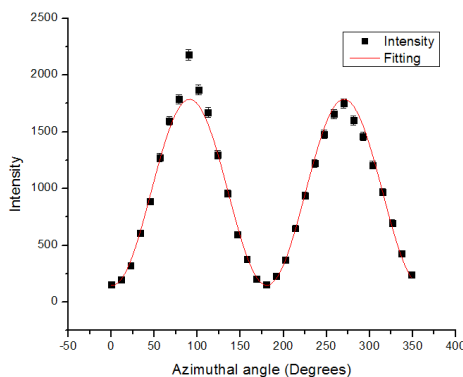

Fig. 9: *Projection of the 2D position distribution for Compton scattering at the angle $\theta = 90° \pm 15°$ on the φ-axis together with the least square fit of Eqn. 5:M = 0.86 ± 0.01.*

We would like to add, that in order to improve results in this experiment the geometry of the detector system has to be optimized. The thick-

ness should be smaller and the width should be equal to the length of the strips in each side. This will provide square pixels and selection of direction. In this case, the contrast of the scattering between two perpenducular directions will be better and hence modulation function M will be higher.

5 Summary

In this report we present an experimental study of Rayleigh scattering for hard X-rays, exploiting a 2D position sensitive Ge(i) detector. A 2D distribution of Rayleigh scattered photons in our microstrip detector has been obtained. Usefulness of the Rayleigh scattering process for X-ray polarimetry is addressed as well. Since the Rayleigh scattering can influence identification of events in Compton polarimetry, its investigation is also important for determination of the accuracy of polarization measurements.

Acknowledgments

References

[1] S. Tashenov, T. Stöhlker, D. Banaś, K. Beckert, P. Beller, H. F. Beyer, F. Bosch, S. Fritzsche, A. Gumberidze, S. Hagmann, et al., Phys. Rev. Lett. **97**, 223202 (2006).

[2] S. Tashenov, A. Khaplanov, B. Cederwall, and K. U. Schässburger, Nuclear Instruments and Methods in Physics Research A **600**, 599 (2009).

[3] S. C. Roy, B. Sarkar, L. D. Kissel, and R. H. Pratt, Phys. Rev. A **34**, 1178 (1986).

[4] U. Spillmann, H. Bräuning, S. Hess, H. Beyer, T. Stöhlker, J.-C. Dousse, D. Protic, and T. Krings, Review of scientific instruments **79**, 83 (2008).

[5] S. Chatterjee, H. F. Beyer, D. Liesen, T. Stöhlker, A. Gumberidze, C. Kozhuharov, D. Banaś, D. Protic, K. Beckert, P. Beller, et al., Nuclear Instruments and Methods in Physics Research B **245**, 67 (2006).